58–68 *Nucleic Acids Research, 2007, Vol. 35, No. 1* *Published online 6 December 2006*
doi:10.1093/nar/gkl948

The chemical stability of abasic RNA compared to abasic DNA

Pascal A. Küpfer and Christian J. Leumann*

Department of Chemistry and Biochemistry, University of Bern, Freiestrasse 3, CH-3012 Bern, Switzerland

Received September 11, 2006; Revised and Accepted October 20, 2006

ABSTRACT

We describe the synthesis of an abasic RNA phosphoramidite carrying a photocleavable 1-(2-nitrophenyl)ethyl (NPE) group at the anomeric center and a triisopropylsilyloxymethyl (TOM) group as 2′-O-protecting group together with the analogous DNA and the 2′-OMe RNA abasic building blocks. These units were incorporated into RNA-, 2′-OMe-RNA- and DNA for the purpose of studying their chemical stabilities towards backbone cleavage in a comparative way. Stability measurements were performed under basic conditions (0.1 M NaOH) and in the presence of aniline (pH 4.6) at 37°C. The kinetics and mechanisms of strand cleavage were followed by High pressure liquid chromotography and ESI-MS. Under basic conditions, strand cleavage at abasic RNA sites can occur via β,δ-elimination and 2′,3′-cyclophosphate formation. We found that β,δ-elimination was 154-fold slower compared to the same mechanism in abasic DNA. Overall strand cleavage of abasic RNA (including cyclophosphate formation) was still 16.8 times slower compared to abasic DNA. In the presence of aniline at pH 4.6, where only β,δ-elimination contributes to strand cleavage, a 15-fold reduced cleavage rate at the RNA abasic site was observed. Thus abasic RNA is significantly more stable than abasic DNA. The higher stability of abasic RNA is discussed in the context of its potential biological role.

INTRODUCTION

Abasic sites are well known DNA lesions that occur spontaneously via depurination at a frequency of ~10 000 per genome per day in mammalian cells (1). Acidic or alkylating conditions as well as oxidative stress greatly enhance this number. Abasic DNA is unstable and undergoes strand cleavage 3′ to the abasic site with an average lifetime of 8 days at 37°C, pH 7.4 and physiological ionic strength (2). Due to the degradation of the genetic material and to missing coding information such sites are highly mutagenic and a major threat to living cells (3,4). Living organisms have therefore evolved a highly efficient and complex DNA repair machinery that maintains genome integrity (5). One component of this machinery is the base excision repair pathway in which abasic sites are produced as intermediates by DNA glycosylases and cleaved either by AP-endonucleases or by AP-lyases. It is only recently that cellular repair processes were also found in RNA. For example, the human oxidative demethylases hABH3 that reverse alkylation of bases in DNA were found to repair also RNA (6). When expressed in *Escherichia coli* they were found to reactivate methylated RNA bacteriophage MS2 *in vivo*. This illustrates the biological relevance of such a repair activity and points towards RNA repair being a potentially important defense mechanism in living cells.

Spontaneous or induced abasic lesions are *a priori* not restricted to DNA but can also occur in RNA. Given the fact that not only short lived mRNA but long-lived tRNAs and ribosomal RNAs are present at all times in a cell in much higher concentrations than DNA, and given also the fact that RNA viruses as well as retroviruses store their genetic information in form of RNA, it is not excluded that abasic RNA plays a significant biological role. Literature about the chemistry and chemical biology of RNA abasic sites is, however, scarce and their biological impact is largely unexplored with a few exceptions. For example, RNA abasic sites are known to be the result of the action of RNA N-ribohydrolases (7). A famous example is the peptide toxin ricin which depurinates a specific adenosine residue on 28S rRNA, one of the RNA chains of eukaryotic ribosomes. This leads to poor binding of elongation factors and knockout of protein synthesis. A single molecule of ricin suffices to kill a whole cell. Besides this there is evidence for a class of RNA specific lyases that act on rRNA abasic sites, leading to complete inactivation of ribosomes (8,9).

Data on the mechanism and kinetics of strand scission of abasic RNA in comparison to abasic DNA is virtually inexistent. *In vitro* generation and cleavage of abasic RNA has been of some interest in the context of RNA sequencing via base alkylation and depurination followed by strand scission induced by aniline under neutral to slightly acidic conditions. It is believed that under these conditions only β-elimination of the phosphate unit on the 3′-side occurs,

*To whom correspondence should be addressed. Tel: +41 31 631 4355; Fax: +41 31 631 3422; Email: leumann@ioc.unibe.ch

leaving behind a 5′-oligonucleotide with a pendent 4,5-dihydroxy-2-oxovaleraldehyde moiety. In another example similar chemistry was used to excise one specific abasic nucleotide out of yeast $tRNA^{Phe}$. Here the intrinsic lability of the glycosidic bond of wybutosine was used to selectively produce one abasic site, followed by treatment with 2-aminopyridine to effect β,δ-elimination, leaving behind 3′ and 5′-phosphorylated ends that were religated in three consecutive enzymatic steps (10).

Given the lack of knowledge on the chemistry and chemical biology of RNA abasic sites we set out to investigate this in more detail. More precisely we synthesized an abasic RNA precursor phosporamidite that carries a photocleavable protecting group at the anomeric center (11). This unit can be introduced into oligoribonucleotides via automated RNA synthesis and the abasic site can be revealed after detachment from solid support and high pressure liquid chromotagraphy (HPLC) purification by photolysis. In preliminary work we reported on the *trans*-lesion synthesis of HIV-1 reverse transcriptase on a RNA-template/DNA-primer system with an abasic site in the RNA template, and on the degradation of the damaged template by the RNase H activity of the polymerase in comparison to a non-damaged template (12). We found efficient incorporation of deoxynucleotides opposite the lesion following the 'A-rule', previously described for DNA-templated *trans*-lesion synthesis (13). Here we present now a detailed analysis of the kinetics and mechanisms of strand cleavage of RNA abasic sites at various conditions in comparison to abasic DNA.

MATERIALS AND METHODS

Synthesis, deprotection and purification of oligonucleotides

Full experimental details on the synthesis of the RNA and DNA abasic site phosphoramidites **1–3** (Scheme 1) containing the photocleavable 1-(2-metyhl)nitrophenethyl (NPE) group is given in the supplementary data section. All oligonucleotides were prepared by automated oligonucleotide synthesis with an Expedite 8909 nucleic-acid synthesis system (PerSepitve Biosystems Inc., Framingham, MA) by using the cyanoethyl-phosphoramidite approach. RNA synthesis was performed with 2′-*O*-TBDMS protected PAC-phosphoramidites (Glen Research Corp., Sterling, VA) on polystyrene solid supports (Amersham Biotech). 2′-OMe-RNA oligoribonucleotides were prepared with benzoyl (A, C) and dimethylformamidino (G) protected 2′-OMe RNA phosphoramidites (Glen Research Corp., Sterling, VA). All 2′-OMe-RNA sequences were synthesized on normal RNA solid supports thus leading to oligonucleotides with an unmodified 3′-terminus. For DNA synthesis benzoyl (dA, dC) and isobutyryl (dG) protected phosphoramidites and controlled pore-glass solid supports (Glen Research Corp., Sterling, VA) were used. The syntheses were performed using the standard coupling protocols for DNA and RNA synthesis, with 5-(ethylthio)-1*H*-tetrazole (*Aldrich*) as activator and a coupling time of 90 s for DNA and 6 min for RNA and 2′OMe-RNA building blocks. The modified phosphoramidites **1–3** were allowed to couple for 6 min and 12 min for DNA and RNA, respectively. Solid supports were treated with $EtOH/NH_4OH$ (1:4) at 55°C, overnight. The DNA and RNA heptamers were purified by using RP-HPLC on an ÄKTA 900 HPLC system (Amersham Pharmacia Biotech). A SOURCE™ 15RPC ST 4.6/100 (polystyrene/divinyl benzene, 15 μm, 100/4.6 mm) column (Amersham Biosciences, Uppsala, Sweden) was used with a linear gradient of solvent A (0.1 M Et_3NOAc in H_2O) and solvent B [0.1 M Et_3NOAc, CH_3CN/H_2O (4:1)]. RNA sequences were further silyl deprotected by treatment with Bu_4NF (1 M in THF) for 16 h at RT. Deprotected oligoribonucleotides were desalted by using Sep-Pak® C_{18} columns (Waters Corp., Milford, MA) before purification by RP-HPLC. Purified oligonucleotides were dissolved in DEPC-treated water and the concentrations of these stock solutions (O.D. 260 nm) were determined with a NanoDrop® ND-100 UV/Vis spectrophotometer (NanoDrop Technologies, Wilmington, DE). All abasic oligonucleotides as well as their NPE-protected precursors were analyzed by ESI-MS.

Strand cleavage kinetics

Sample preparation. Aliquots (0.3 or 0.4 ml of a 1 OD_{260} ml^{-1} solution) of NPE-protected RNA heptamers in H_2O in a quartz cuvette were deprotected at room temperature by using a UV immersion lamp TQ 150 (UV-RS-2, Heraeus) for 2 min. Alternatively, deprotection was achieved using a slide projector with a 250 W tungsten halogen lamp for 6 min. For both methods a conventional glass plate was used as a filter to remove light with wavelengths <300 nm to avoid damage to the oligonucleotides.

Alkaline strand cleavage. Deprotected oligonucleotides were treated with 1 M NaOH to a final concentration of 0.1 M NaOH and incubated at 37°C. Samples were quenched with a stoichiometric amount of 1 M HCl and the reaction mixtures were immediately analyzed by RP-HPLC. The ratio of the remaining abasic heptamer to reaction products was determined by peak integration. The resulting values were fitted with a first order exponential decay using OriginPro 7.5 software (OriginLab Corp., Northhampton, MA). Resulting half-life times $T_{1/2}$ were calculated from the fitted curves that were corrected, where necessary, for the observed amount of products already present at $t = 0$. Alternatively, the $\ln([oligo]/[oligo]_0)$ was plotted against the time t. In all cases a linear relationship was observed, indicating first order kinetics. The first order rate constants for strand scission k_s (s^{-1}) were obtained from the slopes of the respective linear fits.

Strand cleavage in the presence of aniline at pH 4.6. Deprotected oligonucleotides were diluted to a final concentration of 1 OD_{260} ml^{-1} in 0.5 M aniline–HCl, pH 4.6 (0.4 ml). The aliquots are incubated at 37°C for different time intervals. To quench the reactions, aniline was removed by quick DEAE HPLC (Nucleogen® 60-7 125/4 mm column, Macherey–Nagel) with the following gradient: 0% solvent A (0.25 mM Na_2HPO_4 + 0.25 mM NaH_2PO_4 in 20% acetonitrile) for 10 min, 100% solvent B (A + 1 M NaCl) for 5 min. The oligonucleotides eluted with solvent B are collected and carefully concentrated (Speedvac) to a volume of ∼0.4 ml and further analyzed by RP-HPLC as described above.

Fragment identification. Cleavage products of three independent cleavage reactions each were separated by RP-HPLC as described, pooled, lyophilized and analyzed by ESI^- mass

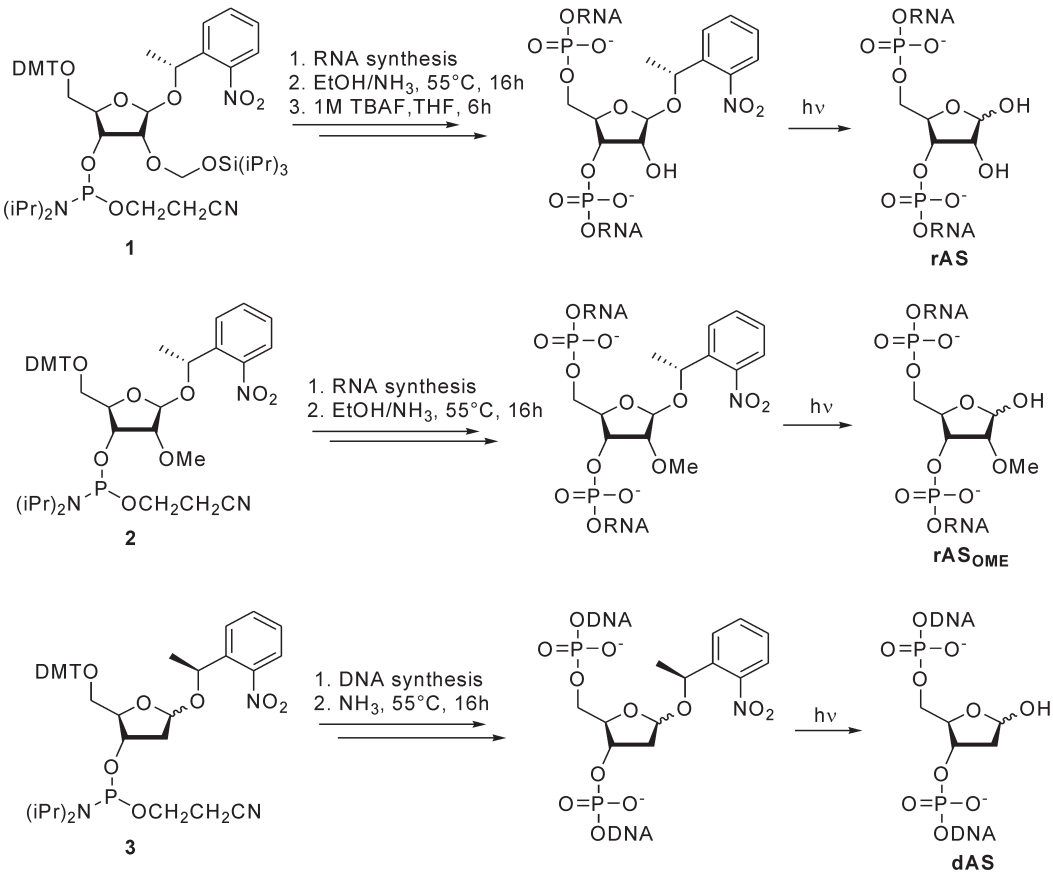

oligonucleotide	+NPE[a]		-NPE[b]	
	a		**b**	
	m/z calc.	m/z found	m/z calc.	m/z found
4 r(AGG-**rAS**-UUC)	2235.4	2236.4	2086.3	2086.3
5 r($A_{OMe}G_{OMe}G_{OMe}$-**rAS$_{OME}$**-$U_{OMe}U_{OMe}$C)	2320.6	2320.1	2171.5	2171.0
6 r($A_{OME}G_{OME}G_{OME}$-**rAS**-$U_{OME}U_{OME}$C)	2306.6	2306.6	2157.4	2157.5
7 d(AGG-**dAS**-TTC)	2151.5	2151.9	2002.3	2002.9

a) Oligonucleotides before NPE deprotection, b) Oligonucleotides after NPE deprotection

Scheme 1. Synthesis and sequences of rAS-, rAS_{OMe}- and dAS-containing oligonucleotide heptamers.

spectrometry. In the case of oligonucleotide **4b** the pooled fragments after aniline removal were desalted over Sep-Pak® C_{18} columns (Waters Corp., Milford, MA) and measured directly by ESI-MS without RP-HPLC separation.

RESULTS

Synthesis of abasic building blocks and oligonucleotides

The synthesis of the RNA and DNA abasic site phosphoramidites **1–3** (Scheme 1) containing the photocleavable 1-(2-nitrophenyl)ethyl (NPE) group, which was used successfully before in oligonucleotide synthesis as protecting group for the 2′-OH function of ribonucleosides (14) or for caging RNA and DNA bases (15–17), is described in the supplementary data section. Their synthesis is straight forward and resulted in overall yields of 21% for the rAS and 32% for the rASOMe phosphoramidite starting from tetraacetyl ribose, as well as 44% for the dAS building block starting from 1,3,5-tri-*O*-acetyl-2′-deoxy-D-ribose. Both configurations at the chiral center of the NPE protecting group were used for reasons of synthetic economy and in both cases photolytic removal was quantitative (see Supplementary Data). These building blocks were stable for more than 1 year when kept in the dark at −20°C. Direct contact to sunlight was avoided but otherwise no special light protection was used during synthesis or manipulation of these abasic site precursors. The synthesis of oligonucleotides was performed

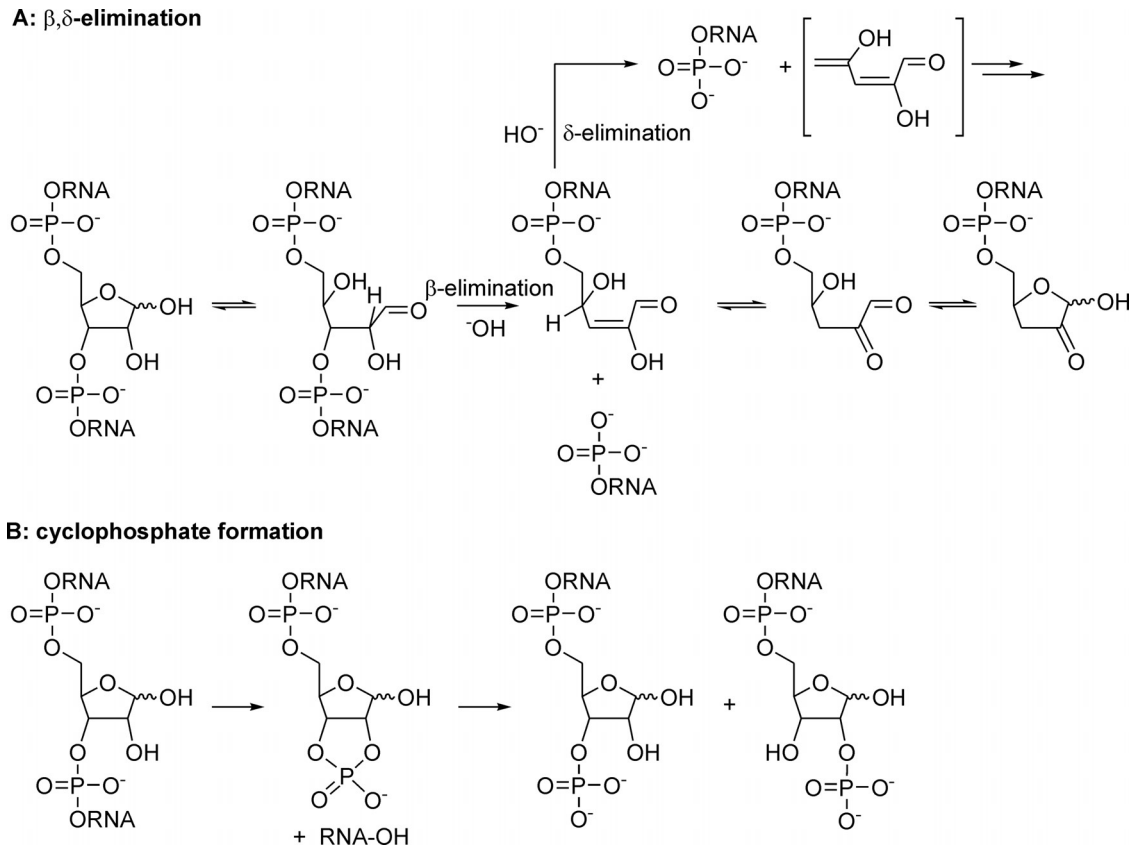

Scheme 2. (**A** and **B**) Mechanisms of strand cleavage of abasic RNA at high pH.

by standard phosphoramidite chemistry (Scheme 1) and resulted in coupling yields for building blocks **1–3** that are in the same range as for natural nucleoside phosphoramidites (>95%). Typically, oligoribonucleotides were HPLC purified before silyl deprotection. We found that this lead to purer oligonucleotide samples after desilylation.

In a first step we determined the deprotection kinetics of the NPE group in the ribonucleotide **4a** at a concentration of 1 OD_{260} ml^{-1} with glass-filtererd light from a UV immersion lamp and followed the progress of deprotection by RP-HPLC at different time intervals. The HPLC traces (see Supplementary Data) showed clean conversion to the AS-containing oligonucleotide **4b** following first order kinetics. The half-life time was calculated to be 12.5 s. Traces of **4b** (<5%) resulting from deprotection during manipulations could already be seen at the beginning. An irradiation time of 2 min was found to be sufficient to achieve almost quantitative deprotection. In an alternative setup we used a slide projector with a halogen lamp for irradiation. Due to its lenses, UV light <365 nm was filtered out. Irradiation times of 6–10 min were found sufficient to promote full NPE-cleavage. This latter method is very mild and was generally preferred in further experiments.

We applied the same NPE-deprotection protocols also to the dAS percursor **7a**. Again we found first order kinetics for NPE deprotection to **7b** with a half-life time of 3.4 s. Long time (~15 min) UV irradiation with the UV lamp lead to a side product that was not identified but that was clearly not the result of strand cleavage. Most likely it is a product resulting from T-T cyclobutane formation. Again irradiation with the slide projector for 5 min effected complete revelation of the abasic site without producing traces of this side product and was therefore considered superior.

Mechanisms of RNA abasic site cleavage

The presence of the 2′-OH group at an RNA- compared to a DNA abasic site substantially influences the mechanism of cleavage at high pH. The structurally and kinetically relevant intermediates for hydroxide induced strand scission are depicted in Scheme 2. As in the case of DNA, β-elimination of the oligonucleotide fragment 3′ to the abasic site can occur from the aldehyde form yielding a 5′-phosphorylated 3′-fragment and an enol intermediate which after enol-ketone tautomerization leads to a 4,5-dihydroxy-2-oxo-valeraldehyde unit attached to the 5′-fragment of the original RNA (Scheme 2A). Alternatively, the enol form is suited to a further δ-elimination step leading to complete excision of the abasic ribose unit and leaving behind a 3′-phosphorylated 5′ end. Besides this an alternative mechanism via cyclophosphate formation (Scheme 2B) does also apply under basic conditions producing a 5′-fragment with an abasic site that is phosphorylated in the 2′ or 3′ position and a 3′-fragment with a 5′-OH end. Cyclophosphate formation must not only occur in the hemiacetal form but can also happen in the aldehyde form of the abasic site (not shown in Scheme 2B).

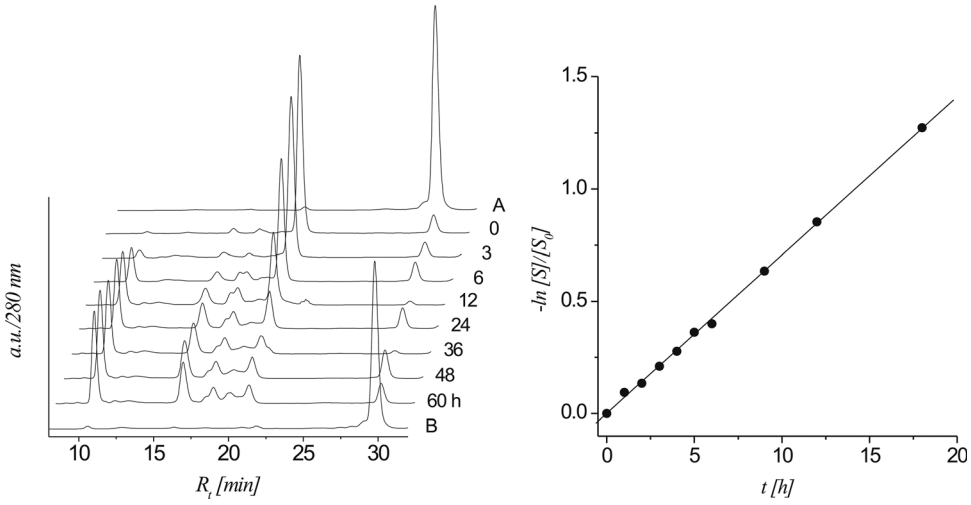

Figure 1. left: HPLC traces (280 nm) of the β-elimination reaction of the 2′-OMe heptamer **5b** at different time intervals; controls: trace A: protected heptamer **5a**; trace B: protected **5a** after treatment with 0.1 M NaOH for 48 h at 37°C; right: linear fit ($R^2 > 0.999$) of $\ln[S]/[S_0]$ versus t calculated from the HPLC traces.

To determine the contribution of each of these mechanisms to overall strand scission we performed separate kinetic analyses with oligonucleotide **5b** and **6a** and compared the results to that of **6b** in which both mechanisms are active simultaneously. In **5b**, the 2′-OH positions are methylated (with the exception of the 3′ terminal C) and the abasic site is deprotected, thus excluding cyclophosphate formation, but admitting β-elimination. In **6a** the abasic site is still NPE protected, while the 2′-position of the abasic ribose is free. Here β-elimination is excluded but cyclophosphate formation at the abasic ribose is allowed. Oligonucleotide **7b** served as the DNA abasic site model that was used for comparison. The kinetics of strand scission was followed by reversed phase HPLC after incubating the oligonucleotides (Na^+ form) with 0.1 M NaOH at 37°C. In regular time intervals samples were injected and the relative amount of residual starting material determined by peak integration. The half-life times ($T_{1/2}$) were calculated from a first order exponential fit while the first order rate constants k_s for strand scission were obtained from the slope of a linear plot of $\ln [S]/[S_0]$ versus t where $[S]/[S_0]$ means the relative amount of unreacted abasic oligonucleotide at the time t.

β,δ-elimination at an RNA abasic site

The time course of strand cleavage of oligonucleotide **5b** is depicted in Figure 1. From the HPLC traces it becomes clear that the abasic heptamer **5b** (peak 4) decreases while at the same time three major fragments with lower retention times appear (peaks 1–3). Lane B is a control with protected oligonucleotide **5a** proving that no cleavage occurs if the anomeric center is still protected. The $T_{1/2}$ and k_s for **5b** under these conditions were calculated to be 594 min and 1.96×10^{-5} s^{-1}, respectively. Peaks 1–3 were isolated and analyzed by ESI-MS (Table 1). Peaks 2 and 3 contain the two 5′-RNA-fragments after β-elimination and β,δ-elimination, respectively, while peak 1 corresponds to the phosphorylated 3′-fragment. Thus it is clear that both β-and δ-elimination steps take place, however at much slower rates compared to DNA **7b** (Table 4).

Table 1. Fragment analysis of cleavage of **5b**

peak	R_t [min]	Structure	Formula	m/z calc.	m/z found
1	10.5	r($pU_{OMe}U_{OMe}C$)	$C_{29}H_{40}N_7O_{24}P_3$	963.60	963.64
2	16.1	r($A_{OMe}G_{OMe}G_{OMe}p$)	$C_{33}H_{44}N_{15}O_{21}P_3$	1079.73	1079.26
3	18.2	r($A_{OMe}G_{OMe}G_{OMe}$prb)[a]	$C_{39}H_{52}N_{15}O_{24}P_3$	1207.86	1207.34

[a]rb = 4,5-dihydroxy-2-methoxy-2-pentenal.

Table 2. Fragment analysis of cleavage of **6a**

Peak	R_t [min]	Structure	Formula	m/z calc.	m/z found
1	11.6	r($U_{OMe}U_{OMe}C$)	$C_{29}H_{39}N_7O_{21}P_2$	883.62	883.20
2	19.5	r($A_{OMe}G_{OMe}G_{OMe}$ASp)	$C_{33}H_{44}N_{15}O_{21}P_3$	1440.98	1440.35
3	20.6	r($A_{OMe}G_{OMe}G_{OMe}$ASp)	$C_{39}H_{52}N_{15}O_{24}P_3$	1440.98	1440.34

Cyclophosphate formation at the RNA abasic site

To study strand scission via cyclophosphate formation independently from β,δ-elimination chemistry, oligonucleotide **6a** was subjected to the same basic conditions and its decay followed again by HPLC (Figure 2).

The HPLC traces show as expected a decrease of peak 4 corresponding to the heptamer **6a** and the appearence of three novel fragments (peaks 1–3) with lower retention times. Trace A shows oligonucleotide **6b** in which the abasic site was deprotected as a control. The absence of this peak in the other traces clearly shows that the 1NPE group is stable under the basic conditions and that no β,δ-elimination can be observed. We calculated again the $T_{1/2}$ for the disappearance of **6a** as described before and found a value of 221 min k_s in this case was found to be 5.95×10^{-5} s^{-1}.

To follow the mechanism of cleavage we isolated the newly arising peaks 1–3 and analyzed the RNA fragments by ESI-MS (Table 2). Peak 1 contains the 3′-RNA fragment with a free 5′-OH group which is in accord with hydrolysis via cyclophosphate formation. Peaks 2 and 3 both contain fragments with the same mass that correspond to the isomeric 5′-fragment in which the terminal phosphate group is located

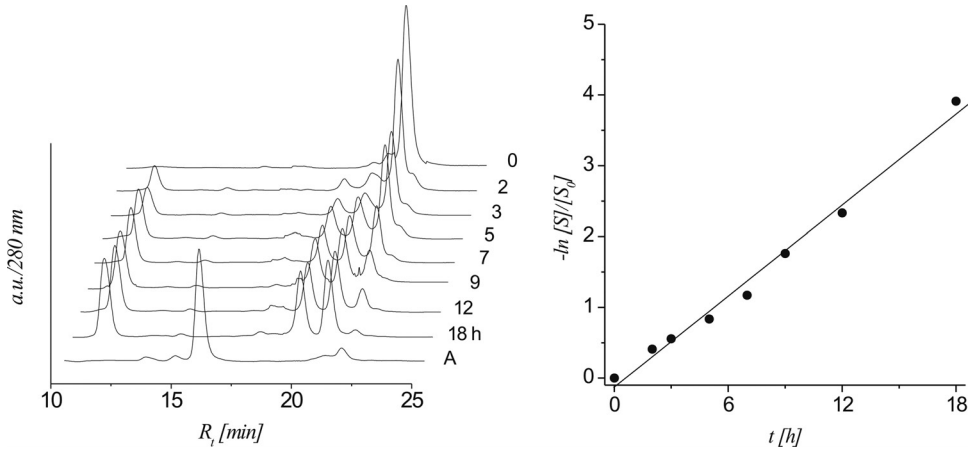

Figure 2. HPLC left: traces of strand cleavage via cyclophosphate formation of **6a** (0.1 M NaOH, 37°C) at different time intervals; controls: trace A: oligomer **6b**; right: linear fit ($R^2 > 0.994$) of ln[*S*]/[S_0] versus *t* calculated from the HPLC traces.

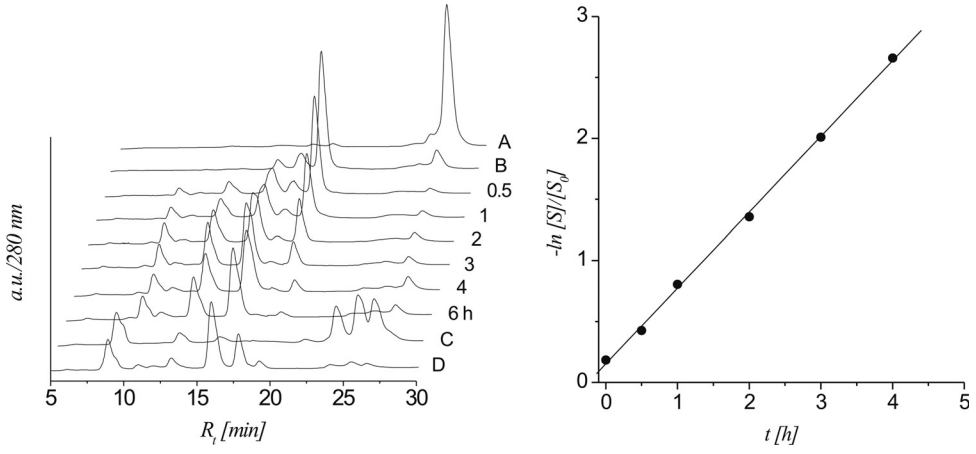

Figure 3. left: HPLC traces of strand cleavage via cyclophosphate formation and β,δ-elimination of **6b** (0.1 M NaOH, 37°C) at different time intervals; controls: trace A: **6a**, trace B: **6b**, trace C: **6a** (0.1 M NaOH, 6.5 h, 37°C), trace D: **6a** (0.1 M NaOH, 6.5 h, 37°C, followed by photolysis); right: linear fit ($R^2 > 0.999$) of ln[*S*]/[S_0] versus *t* calculated from the HPLC traces.

either at O2′ or O3′. The corresponding cyclophosphate intermediate could not be isolated in this case.

Combination of β,δ-elimination and cyclophosphate formation in strand cleavage at the RNA abasic site

Since the two strand cleavage mechanisms studied separately so far act in concert in abasic RNA, it was necessary to study the effect of their combination on strand cleavage efficiency. For this purpose oligonucleotide **6b** was subjected to 0.1 M NaOH and strand cleavage analyzed as described before (Figure 3).

Olignucleotide **6b** disappears under standard basic conditions with a $T_{1/2}$ of 69 min and a k_s of 1.73×10^{-4} s^{-1} as can be seen from the fit. This is considerably faster compared to **6a** and **6b** and is due to the overlay of the two mechanisms for strand scission (Table 4). A calculated $T_{1/2}$ for **6b** from those of **5b** and **6a** resulted in a value of 165 min. The difference between calculated and measured value is in reasonable agreement and validates the 2′-OMe modification as a model for studying the β-elimination mechanism.

The overlay of the two modes for strand cleavage gives rise to an increased number of fragments. Fractions of the newly arising three main peaks (peaks 1–3) in the HPLC were again isolated and subjected to fragment analysis (Table 3). To have a first indication weather cyclophosphate formation would be dominant, protected heptamer **6a** was also submitted to basic conditions (0.1 M NaOH at 37°C, 6.5 h, trace C) and deprotected afterwards (trace D). Fraction 1 contained the 5′-phosphorylated 3′-fragment of **6b** arising from β,δ-elimination while fraction 2 contained the corresponding non-phophorylated fragment which is expected from strand scission via cyclophosphate formation. The MS spectrum of fraction 3 revealed four major signals from four different fragments which could be identified as the 3′-phosphorylated 5′-fragment of **6b** together with that with the pending 4,5-dihydroxy-2-oxo-pentanal residue, arising from β,δ- and β-elimination, respectively. A second set of signals could be attributed to the same RNA fragment with the abasic ribose unit in its cyclophosphate and its hydrolyzed phosphate form. These products clearly arise from the hydrolytic strand scission pathway. Thus, fragment analysis clearly proves that both strand scission mechanisms are simultaneously active

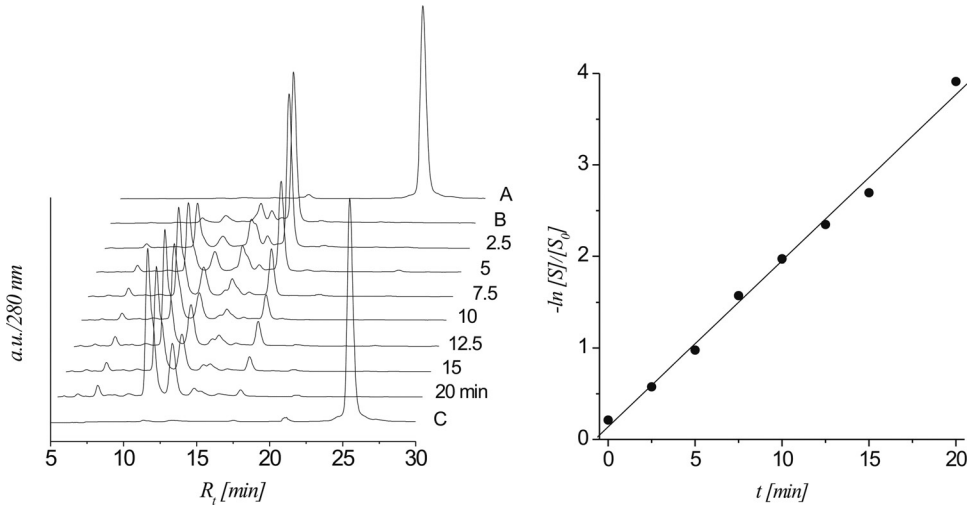

Figure 4. left: HPLC traces of strand cleavage via β,δ-elimination of **7b** (0.1 M NaOH, 37°C) at different time intervals; controls: trace A: **7a**; trace B: **7b**; trace C: **7a** after treatment with 0.1 M NaOH, 37°C for 20 min; right: linear fit ($R^2 > 0.996$) of $\ln[S]/[S_0]$ versus t calculated from the HPLC traces.

Table 3. Fragment analysis of strand scission of **6b**

Nr	R_t (min)	Fragment[a]	Formula	m/z calc.	m/z found
1	10.3	r(p$U_{OMe}U_{OMe}$C)	$C_{29}H_{40}N_7O_{24}P_3$	963.60	963.26
2	13.6	r($U_{OMe}U_{OMe}$C)	$C_{29}H_{39}N_7O_{21}P_2$	883.62	883.22
3	16.2	r($A_{OMe}G_{OMe}G_{OMe}$p)	$C_{33}H_{44}N_{15}O_{21}P_3$	1079.73	1079.34
		r($A_{OMe}G_{OMe}G_{OMe}$-rb)	$C_{38}H_{52}N_{15}O_{25}P_3$	1211.85	1211.51
		r($A_{OMe}G_{OMe}G_{Ome}$AScp)	$C_{38}H_{51}N_{15}O_{27}P_4$	1273.81	1273.36
		r($A_{OMe}G_{OMe}G_{OMe}$ASp)	$C_{38}H_{53}N_{15}O_{28}P_4$	1291.83	1291.34

[a]rb = 4,5-dihydroxy-2-oxo-pentanal, cp = 2′,3′-cyclophosphate, AS = abasic residue.

and contribute to the observed faster overall rate of strand cleavage as compared to **5b** and **6a**.

β,δ-elimination at a DNA abasic site

To compare the relative stability of the RNA abasic site with its DNA analogue, the abasic DNA heptamer **7b** was prepared and subjected to basic degradation under the same conditions (0.1 M NaOH, 37°C). The mechanism and kinetics of decay were measured as described before (Figure 4).

Oligodeoxynucleotide **7b** rapidly degrades into at least one intermediate and two stable products with a $T_{1/2}$ of only 4.1 min and a k_s of 3.02×10^{-3} s^{-1}. HPLC analysis indicated the d(pTTC) fragment (m/z = 915.15) to be the faster eluting and d(AGGp) (m/z = 989.38) to be the slower eluting fragment, both being the expected products of β,δ-elimination. We assume that the transiently formed intermediate corresponds to the 5′-DNA fragment after β-elimination with the pending 4,5-dihydroxypent-2-enal unit but we did not investigate this in further detail.

For an overview of abasic site decay under alkaline conditions, all measured first order rate constants and the corresponding half-life times were summarized in Table 4, together with k_{rel}, indicating relative differences in the rates of abasic site cleavage. It becomes immediately evident that β,δ-elimination at a DNA abasic site is 154-fold faster than at an RNA abasic site. This highlights the strong influence of the 2′-OH group on this mechanism for strand scission. Interestingly, strand cleavage via cyclophosphate formation is 3-fold faster compared to strand cleavage via β,δ-elimination in RNA. In the case of an unperturbed abasic site, where both mechanisms can contribute to strand clavage, the RNA abasic site shows ∼16-fold enhanced stability compared to a DNA abasic site.

Aniline mediated strand cleavage at pH 4.6

It is long known that strand cleavage of abasic DNA at physiological ionic strength and neutral to slightly acidic pH is greatly enhanced in the presence of amines (2). It was therefore of interest to investigate strand cleavage of abasic RNA in the presence of an amine and compare it to DNA. We have chosen aniline as a model amine because abasic RNA cleavage by this amine at pH 4.6 was used in the past for sequencing and site specific modification of RNA (10,18). A potentially simplified mechanism for the aniline mediated abasic RNA decay is given in Scheme 3.

It is beyond doubt that strand cleavage is initiated by immonium ion formation which renders the 2′-H base-labile and the 3′-phosphate unit prone to β-elimination. The intermediate enol strongly prefers the keto tautomeric form which renders δ-elimination that could in principle be initiated via vinylogous deprotonation of 4′-H slow. Given the fact that strand cleavage occurs in a slightly acidic medium, concomittant cyclophosphate formation, as observed under under alkaline conditions, is no longer obscuring β-elimination and for this reason the following experiments were performed with the 2′-unmodified abasic RNA oligonucleotide **4b**. Again, abasic DNA **7b** was used for comparison. The extent of cleavage was followed also in this case by HPLC (Figures 5 and 6). $T_{1/2}$ and the apparent first order rate constant for strand scission k_s were determined as described before. We found a $T_{1/2}$ of 14 min and a k_s of 8.56×10^{-4} s^{-1} for the abasic RNA **4b**. The control experiments at neutral pH (Figure 5, trace B and C) clearly show that strand cleavage is much slower in the absence of aniline and essentially does not progress significantly over the time

Table 4. Summary of the $T_{1/2}$ and k_s and k_{rel} data measured for alkaline induced strand scission of the abasic RNA and DNA heptamers

	Oligonucleotide			
Abasic site	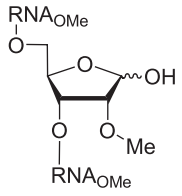 **5b**	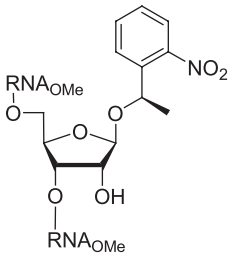 **6a**	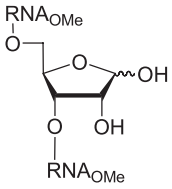 **6b**	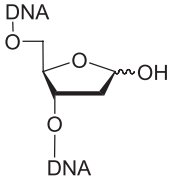 **7**
Mechanism of strand scission	β,δ-elimination	cyclophosphate formation	β,δ-elimination + cyclophosphate formation	β,δ-elimination
$T_{1/2}$ (min)	594	221	69	4.1
k_s (s^{-1})	1.96×10^{-5}	5.95×10^{-5}	1.73×10^{-4}	3.02×10^{-3}
k_{rel}	1	3	9	154

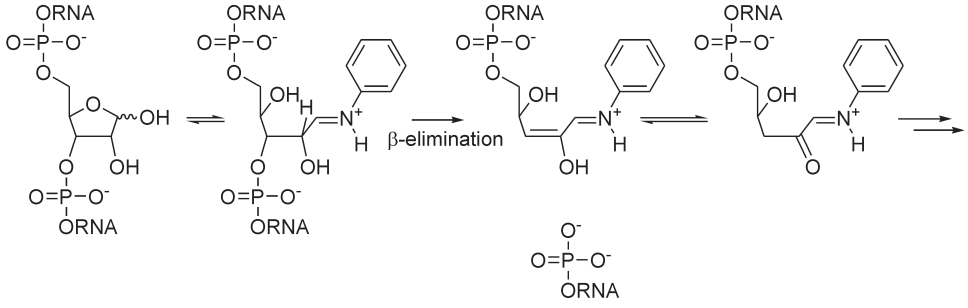

Scheme 3. Structurally and kinetically relevant intermediates in the aniline mediated strand scission at RNA abasic sites at slightly acidic pH.

course of the experiment. The same analysis in the case of the DNA abasic oligomer **7b** resulted in a $T_{1/2}$ of 53 s and a k_s of 1.29×10^{-2} s^{-1}. Also, here strand cleavage in the absence of aniline was negligible over the time course of the experiment (Figure 6, trace B and C).

Fragment analysis in the case of aniline induced strand cleavage by ESI-MS proved more difficult than in the case of base induced cleavage for a yet unknown reason. We were unable to obtain masses for cleavage products in all isolated fractions. Those that could be identifed for **4b** and **7b** were listed in Table 5. In both cases, the trimers 3′ to the abasic sites, as expected from β-elimination, were identified. Interestingly, in the case of the deoxyoligonucleotide **7b**, the 5′-fragment containing the absic residue bound to aniline as well as the aniline adduct of the intact abasic heptamer could be identified. This is a direct proof of the intermediacy of imines or hemiaminals in the cleavage mechanism.

From these experiments, it becomes clear that amines greatly accelerate strand cleavage near neutral pH also in abasic RNA. But again, abasic DNA is cleaved 15-fold faster. If one compares the k_s values of cleavage via β-elimination in the presence of aniline with those obtained for alkaline cleavage it becomes clear that a DNA abasic site is only cleaved 4-fold faster while a RNA abasic site decays 42-fold faster. Thus the 2′-OH group seems to increase the β-elimination chemistry next to the immonium group.

DISCUSSION

We describe here the first direct comparison of the chemical stability of an RNA versus a DNA abasic site under basic conditions and under slightly acidic conditions in the presence of an amine. While under basic conditions no other mechanism than β-elimination is operative in DNA, the situation is more complex in the case of RNA, where cyclophosphate formation is acting in concert with β-elimination. In order to analyze the contribution of each mechanism to strand scission separately we used a 2′-OMe abasic site analogue, incapable of cyclophosphate formation, and a 1′-protected abasic RNA analogue incapable of β-elimination as well as a true abasic site within a 2′-OMe-oligoribonucleotide.

An initial concern was whether the 2′OMe-RNA abasic site analogue would be an adequate model reflecting correctly the β-elimination properties of a true RNA abasic site. This was a *priori* not clear as e.g. reversible, competitive deprotonation at 2′-OH or the shift of the keto function from C1′ to C2′ via a C1′–C2′dienolate could interfere with β-elimination kinetics (Figure 7).

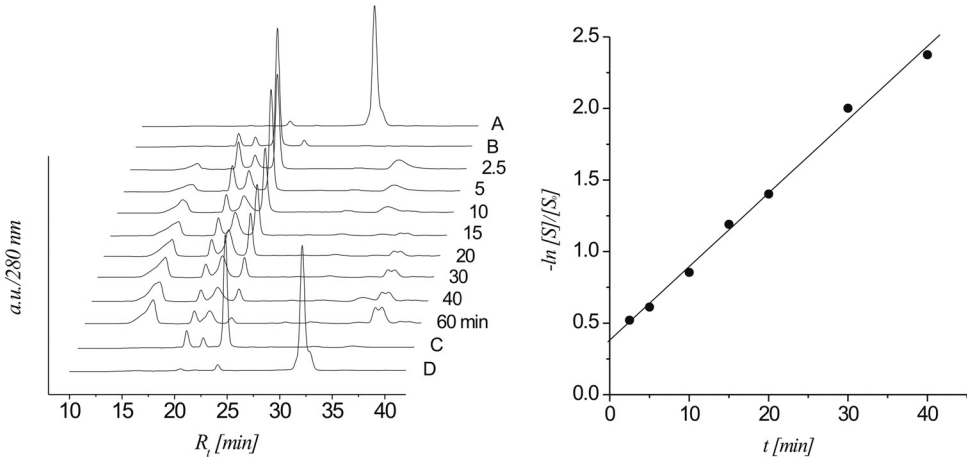

Figure 5. left: HPLC traces of aniline-induced strand cleavage reaction of **4b** at the given time intervals; controls: trace A: protected heptamer **4a**; trace B: deprotected heptamer **4b**; trace C: **4b** after 60 min in 0.3 M TEAA buffer, pH 7.0 at 37°C in the absence of aniline; trace D: protected heptamer **4a** after treatment with aniline for 60 min; right: linear fit ($R^2 > 0.997$) of the $\ln[S]/[S_0]$ versus t for **4b**.

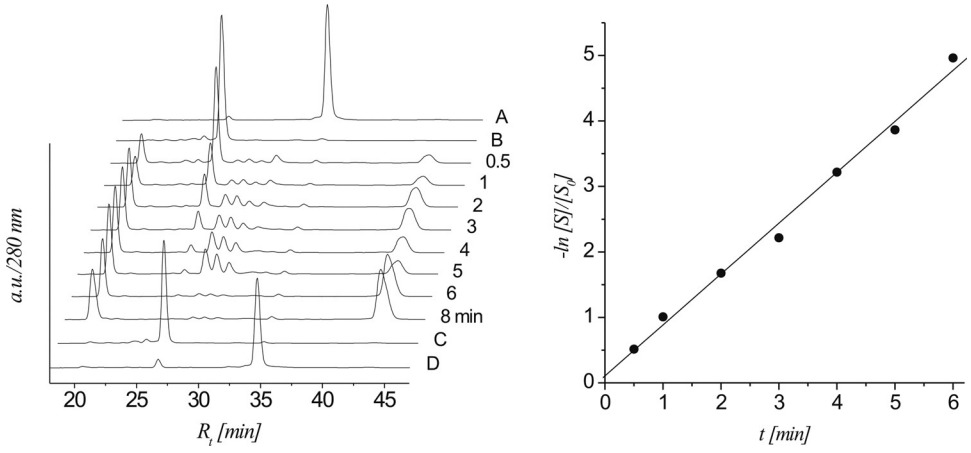

Figure 6. left: HPLC traces of aniline-induced strand cleavage reaction of **7b** at the given time intervals; controls: trace A: protected heptamer **7a**; trace B: deprotected heptamer **7b**; trace C: deprotected heptamer **7b** after 10 min in 0.3 M TEAA buffer, pH 7.0 at 37°C in the absence of aniline; trace D: protected heptamer **7a** after treatment with aniline for 10 min; right: linear fit ($R^2 > 0.996$) of the $\ln[S]/[S_0]$ versus t for **7b**.

Table 5. Identified fragments of aniline induced cleavage at pH 4.6 of oligonucleotides **4b** and **7b**

oligonucleotide	R_t (min)	Identified fragments[a]	Formula	*m/z* calc.	*m/z* found
7b	16.5	r(UUC)	$C_{27}H_{35}N_7O_{21}P_2$	855.6	855.1
	20.3	r(pUUC)	$C_{27}H_{36}N_7O_{24}P_3$	953.5	935.1
4b	20.5	d(pTTC)	$C_{29}H_{40}N_7O_{21}P_3$	915.6	915.2
	20.5	d(TTC)	$C_{29}H_{39}N_7O_{18}P_2$	835.6	835.2
	28.3–30.3	d(AGG)-AS-NHC_6H_5	$C_{41}H_{48}N_{16}O_{19}P_3$	1161.9	1162.3
		d(AGG-AS-NHC_6H_5-TTC)	$C_{70}H_{88}N_{23}O_{40}P_6$	2077.4	2077.4

[a]AS-NHC_6H_5 = imine or hemiaminal between the abasic site and aniline.

We compared therefore $T_{1/2}$ of **6b** with that calculated from the sum of the measured exponential decays of **6a** and **5b**. We found a theoretical $T_{1/2}$ of 165 min which is 2.5-fold longer than that measured for **6b**. From this we conclude that O2′-methylation slightly but not significantly retards β-elimination in abasic RNA which validates the O2′-methylated ribose unit as abasic site model. At the same time this comparison also validates the NPE protected abasic RNA unit with a free 2′-OH group to be a valid model. In a true RNA abasic site not only the hemiacetal form but also the open chain, aldehyde form can undergo strand cleavage via the cyclophosphate pathway. The above described comparison underlines that if this is the case there is either no significant difference in the velocity of cyclophosphate

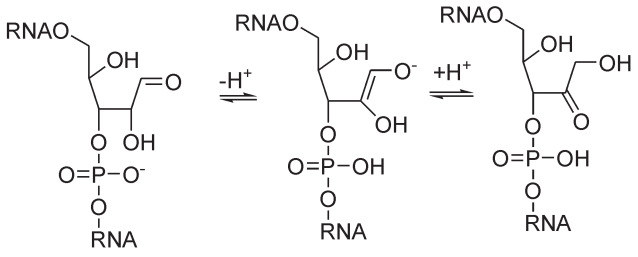

Figure 7. 1′,2′-shift of keto function via a dienolate intermediate.

formation between the open chain and the furanose form, or the open chain form is kinetically not relevant. By comparing the relative rate of strand cleavage we noted that cleavage via cyclophosphate formation is ca 3-fold faster than cleavage by β-elimination. Extrapolated to longer RNA as, e.g. viral RNA this means that under basic conditions strand scission via cyclophosphate formation is clearly the dominant mechanism of decay even in the presence of an abasic site.

From the mechanistic point of view by far the most challenging fact is the roughly 150-fold higher stability of an RNA absic site towards β-elimination compared to DNA under alkaline conditions. Several factors could be responsible for this. A thermodynamic argument would invoke differences in the pKa of the C2′-H as a function of the presence or absence of an OH function. We calculated the C2′-H acidity of a DNA and RNA abasic site model using the SPARC calculator (19) and found only minor differences in pKa (Figure 8A). According to theory, the C2′-H of the RNA abasic site is slightly less acidic compared to DNA but the ΔpKa of only 0.34 can not explain the differences in reactivity. Also retardation of β-elimination via competitive, reversible deprotonation of the 2′-OH group can be excluded as the reason due to the fact that the corresponding 2′-OMe derivative shows slightly slower strand scission kinetics as compared to the non-methylated abasic residue. Also to be excluded are statistical effects resulting from 2 scissile C2′-H bonds in DNA compared to only one in RNA, as this certainly does not explain a more than 150-fold rate difference.

The origin of the stability differences could in principle arise from differential stereoelectronic effects in a concerted *trans*-β-elimination mechanism (Figure 8B). The conformer for which less reactivity of RNA over DNA can be expected is that with the anti-arrangement of the C2′–C3′-bond (Figure 8B, right). Although steric arguments favor this conformation, stereoelectronic effects disfavor this arrangement in the case of RNA due to the anti-alignment of the C2′–O- and the C3′–O-bond, violating the gauche effect. Thus, there is no strong stereoelectronic argument in support of the higher reactivity of a DNA over RNA abasic site.

If one assumes that β-elimination follows a polar, nonconcerted pathway, another hypothesis opens up. Under the basic conditions applied it seems likely that C2′–H dissociation is fast and reversible and therefore dissociation of the C3′–O3′ bond is rate determining. An important role has then to be attributed to the C2′–O2′ σ-bond in RNA which renders dissociation of the C3′–O3′ bond more difficult compared to the C2′–H bond in DNA due to less hyperconjugative stabilization of the transition state upon progressing

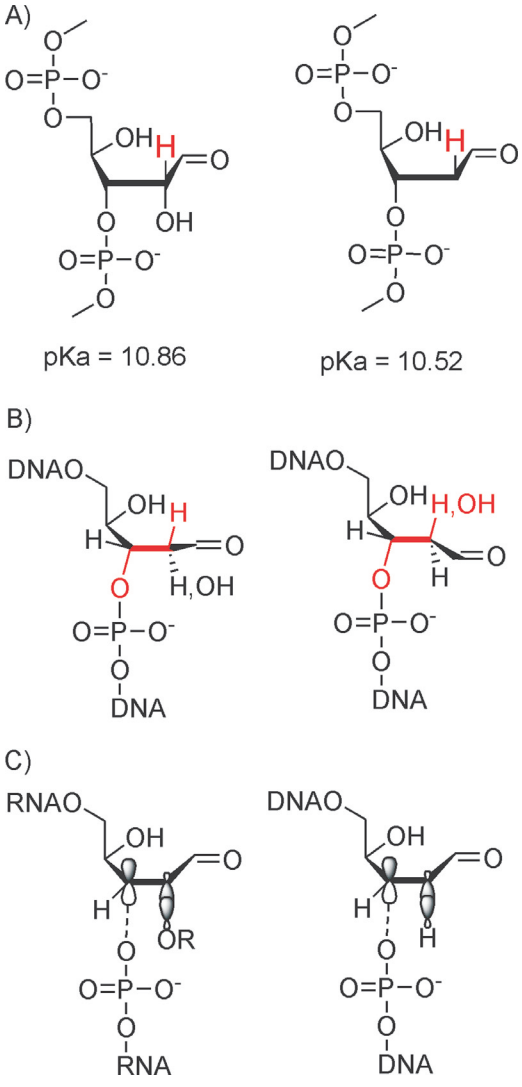

Figure 8. (**A**) C2′–H acidities of an RNA and a DNA abasic site in the aldehyde form; (**B**) syn and anti conformers at the C2′–C3′–bond and implications on the concerted *trans*-β-elimination process for RNA and DNA; (**C**) Model of differential hyperconjugative assistance of C3′–O3′ bond dissociation by a C2′–H or C2′–OH σ-bond in a DNA and RNA abasic site.

C3′–O3′ bond dissociation (Figure 8C). We currently favor this hypothesis as it is in agreement with our experimental observations.

In the Schiff-base induced β-elimination at pH 4.6, the relative rates of cleavage between an RNA and a DNA abasic site are less different. Under these conditions, abasic RNA is still 15-fold more stable compared to abasic DNA. It may well be that under these conditions the deprotonation of the 2′C–H becomes kinetically more dominant compared to the C3′–O3′ bond dissociation in the overall β-elimination mechanism due to the increased difference of the pH of the medium compared to the pKa of the C2′–H. Thus the differences in kinetics between RNA and DNA decay are expected to correlate with the differences of the pKa of the respective C2′–H which is at least qualitatively the case. As a bottom line it appears that also under these more biorelevant conditions there is an advantage in stability of abasic RNA over abasic DNA.

The relative stability of abasic RNA may have interesting biological consequences for long lived RNAs. It is known that spontaneous generation of abasic RNA is slower compared to DNA (20), but once such lesions are formed, their potential biological effect is expected to be higher due to their relative longevity. Ribosome inactivating proteins (RIPs) are long known, but only recently it was found that class-I RIPs such as the pokeweed antiviral protein can not only depurinate the sarcin/ricin loop of the large rRNA but also specific adenine and guanine residues throughout the sequence of capped mRNAs (21) or other viral RNAs (22). This means that there exist not only spontaneous but also enzymatic pathways for abasic mRNA generation. It will therefore be of interest to study the effect of abasic RNA sites on the translation process in more detail.

Another open question associated with RNA abasic sites in long-lived RNA is whether they have any impact on the evolution of viral RNA. In preliminary experiments we studied the *trans*-lesion synthesis of an abasic RNA template/DNA-primer system by HIV-1 reverse transcriptase and found efficient insertion of purine bases opposite the lesion (12). Thus it is not excluded that abasic RNA also contributes to mutations in viral or retroviral RNA during replication or reversed transcription, in addition to the error rate of RNA dependent RNA polymerases (23) or reversed transcriptases (24).

Finally it will be of interest to find out whether there exists a primitive cellular repair system for abasic RNA. There is a growing list of genes involved in RNA damage control (25,26), and it is assumed that many of them are not yet discovered. There is also evidence that defects in the RNome stability might play a role in cancer formation. The study of mRNA biogenesis over the last years lead to the insight that there exists an elaborate RNA quality control mechanism involving, e.g. proteins that select aberrantly spliced mRNAs and mRNAs with premature termination codons (26). mRNAs are the working copies of the genomic information and a cell should therefore have a great investment in maintaining the integrity of its RNA. So, why should there not be a specific mechanism for dealing with abasic RNA? It could be as simple as just a mechanism for inactivating and metabolizing abasic RNA.

SUPPLEMENTARY DATA

Supplementary Data are available at *NAR* Online.

ACKNOWLEDGEMENTS

Financial support from the Swiss National Science Foundation (grant No. 200020-107692) is gratefully acknowledged. Funding to pay the Open Access publication charges for this article was provided by Swiss National Science Foundation.

Conflict of interest statement. None declared.

REFERENCES

1. Lindahl,T. and Nyberg,B. (1972) Rate of depurination of native deoxyribonucleic acid. *Biochemistry*, **11**, 3610–3618.
2. Lindahl,T. and Andersson,A. (1972) Rate of chain breakage at apurinic sites in double-stranded deoxyribonucleic acid. *Biochemistry*, **11**, 3618–3623.
3. Loeb,L.A. and Preston,B.D. (1986) Mutagenesis by apurinic/apyrimidinic sites. *Ann. Rev. Genet.*, **20**, 201–230.
4. Lhomme,J., Constant,J.F. and Demeunynck,M. (1999) Abasic DNA structure, reactivity and recognition. *Biopolymers*, **52**, 65–83.
5. Scharer,O.D. (2003) Chemistry and biology of DNA repair. *Angew. Chem. Int. Ed. Engl.*, **42**, 2946–2974.
6. Aas,P.A., Otterlei,M., Falnes,P.O., Vagbo,C.B., Skorpen,F., Akbari,M., Sundheim,O., Bjoras,M., Slupphaug,G., Seeberg,E. *et al.* (2003) Human and bacterial oxidative demethylases repair alkylation damage in both RNA and DNA. *Nature*, **421**, 859–863.
7. Schramm,V.L. (1997) Enzymatic N-riboside scission in RNA and RNA precursors. *Curr. Opin. Chem. Biol.*, **1**, 323–331.
8. Ogasawara,T., Sawasaki,T., Morishita,R., Ozawa,A., Madin,K. and Endo,Y. (1999) A new class of enzyme acting on damaged ribosomes: ribosomal RNA apurinic site specific lyase found in wheat germ. *EMBO J.*, **18**, 6522–6531.
9. Ozawa,A., Sawasaki,T., Takai,K., Uchiumi,T., Hori,H. and Endo,Y. (2003) RALyase; a terminator of elongation function of depurinated ribosomes. *FEBS Lett.*, **555**, 455–458.
10. Nishikawa,Y., Adams,B.L. and Hecht,S.M. (1982) Chemical excision of apurinic acids from rna. a structurally modified yeast $tRNA^{Phe}$. *J. Am. Chem. Soc.*, **104**, 326–328.
11. Trzupek,J.D. and Sheppard,T.L. (2005) Photochemical generation of ribose abasic sites in RNA oligonucleotides. *Org. Lett.*, **7**, 1493–1496.
12. Kuepfer,P.A. and Leumann,C.J. (2005) RNA abasic sites: preparation and *trans*-lesion synthesis by HIV-1 reverse transcriptase. *Chem. Bio. Chem.*, **6**, 1970–1973.
13. Strauss,B.S. (1991) The 'A rule' of mutagen specificity: a consequence of DNA polymerase bypass of non-instructional lesions? *Bioessays*, **13**, 79–84.
14. Pitsch,S., Weiss,P.A., Wu,X., Ackermann,D. and Honegger,T. (1999) Fast and reliable automated synthesis of RNA and partially 2′-O protected precursors ('caged RNA') based on two novel orthogonal 2′-O protecting groups. *Helv. Chim. Acta*, **82**, 1753–1761.
15. Wenter,P., Furtig,B., Hainard,A., Schwalbe,H. and Pitsch,S. (2005) Kinetics of photoinduced RNA refolding by real-time NMR spectroscopy. *Angew. Chem. Int. Ed. Engl*, **44**, 2600–2603.
16. Wenter,P., Furtig,B., Hainard,A., Schwalbe,H. and Pitsch,S. (2006) A caged uridine for the selective preparation of an RNA fold and determination of its refolding kinetics by real-time NMR. *Chembiochem*, **7**, 417–420.
17. Heckel,A. and Mayer,G. (2005) Light regulation of aptamer activity: an anti-thrombin aptamer with caged thymidine nucleobases. *J. Am. Chem. Soc.*, **127**, 822–823.
18. Rajbhandary,U.L. (1980) Recent developments in methods for RNA sequencing using *in vitro* 32P-labeling. *Fed. Proc.*, **39**, 2815–2821.
19. Hillal,S.H., Karickhoff,S.W. and Carreira,L.A. (1995) A rigorous test for SPARC's chemical reactivity models: estimation of more than 4300 ionization pK(a)s. *Quant. Struct. -Act. Relat.*, **14**, 348–355.
20. Kochetkov,N.K. and Budovskii,E.I. (1972) Hydrolysis of N-glycosidic bonds in nucleosides, nucleotides and their derivatives. In Kochetkov,N.K. and Budovskii,E.I. (eds), *Organic Chemistry of Nucleic Acids*. Plenum, New York, pp. 425–448.
21. Hudak,K.A., Bauman,J.D. and Tumer,N.E. (2002) Pokeweed antiviral protein binds to the cap structure of eukaryotic mRNA and depurinates the mRNA downstream of the cap. *RNA*, **8**, 1148–1159.
22. Parikh,B.A. and Tumer,N.E. (2004) Antiviral activity of ribosome inactivating proteins in medicine. *Mini. Rev. Med. Chem.*, **4**, 523–543.
23. Castro,C., Arnold,J.J. and Cameron,C.E. (2005) Incorporation fidelity of the viral RNA-dependent RNA polymerase: a kinetic, thermodynamic and structural perspective. *Virus Res.*, **107**, 141–149.
24. Menendez-Arias,L. (2002) Molecular basis of fidelity of DNA synthesis and nucleotide specificity of retroviral reverse transcriptases. *Prog. Nucleic Acid Res. Mol. Biol.*, **71**, 91–147.
25. Bregeon,D. and Sarasin,A. (2005) Hypothetical role of RNA damage avoidance in preventing human disease. *Mutat. Res.*, **577**, 293–302.
26. Bellacosa,A. and Moss,E.G. (2003) RNA repair: damage control. *Curr. Biol.*, **13**, R482–R484.